

Effect of molecular packing on the solid state spectra of ruthenium phthalocyanine: anomalous behaviour of a monodimensional stacked assembly

Lucilla Alagna, Aldo Capobianchi, Maria Pia Casaletto, Giulia Mattogno, Anna Maria Paoletti, Giovanna Pennesi and Gentilina Rossi*

Istituto di Chimica dei Materiali, Consiglio Nazionale delle Ricerche, P.O. Box 10, I-00016 Monterotondo, Stazione, Italy. E-mail: rossi@milib.cnr.it

Received 2nd January 2001, Accepted 12th April 2001
First published as an Advance Article on the web 24th May 2001

The ruthenium phthalocyanine molecule has never been isolated as a single unit in the solid phase. Any attempt to obtain it leads to the dimeric form $(\text{RuPc})_2$ with a double bond between Ru–Ru atoms. Owing to the amorphous nature of this compound, its structural characterisation was previously investigated by LAXS (Large Angle X-ray Scattering) and EXAFS (Extended X-ray Absorption Fine Structure) studies. Magnetic and conductivity properties were also discussed in the light of the found structure. The optical spectra of the material in the solid phase and as evaporated films are reported in the present contribution. The obtained results show a marked red shifting absorption when passing from solution to film. Such anomalous behaviour can be explained taking into account the considerable molecular distortion presented by the two macrocycles within the dimer and, overall, considering the strong π – π interactions throughout the molecular stack. The attempt to apply the coupling exciton theory in order to clarify the optical data was not successful for the molecular assembly assumed by $(\text{RuPc})_2$ dimeric units. The EXAFS investigation on films, which supports the suggested interpretation, also shows some degree of flexibility of the molecule which somehow influences the whole molecular packing. Depth profile analysis of $(\text{RuPc})_2$ films, studied by the XPS (X-ray Photo-emission spectroscopy) technique, clearly indicates a homogeneity and a stable chemical composition throughout the thickness.

Introduction

Molecular materials based on phthalocyanine units ($\text{Pc} = \text{phthalocyaninato dianion } \text{C}_{32}\text{H}_{16}\text{N}_8$) have been extensively studied in consideration of the wide range of applications where their particular physico-chemical properties could be exploited. Deposited as thin films they are of great interest for their electrical and optical, even non-linear optical, properties.¹ However, an in-depth study of the structural, spectroscopic and morphological characteristics of the phthalocyanine films will be necessary for any further application as the different polymorphic phthalocyanines exhibit different performances. In fact it is well known that several types of molecular assembly can be expected for phthalocyanines in the solid state² and that characteristic spectral features can be predicted in relation to these assemblies. Many authors^{3–5} have demonstrated the relationship between the different crystal packing present in different polymorphic forms and the observed optical and infra-red (IR) spectra, principally on microcrystalline films of PcH_2 and $\text{PcM}(\text{n})$. However, a coherent pattern of data is not always attained due to the slight differences in polymorphism shown by phthalocyanines. The IR spectra differ slightly in the region $700\text{--}800\text{ cm}^{-1}$ corresponding to the out-of-plane C–H bending of the benzene rings,⁶ while the visible spectra show red or blue shifts of the positions of the typical bands (Q and Soret B bands) of phthalocyanines in solution. In addition, a general broadening and/or splitting of the bands is observed. The theory of the molecular exciton was widely used to rationalise the differences between the optical spectra in the liquid phase and those in the solid phase.⁷

In contrast, very few data exist on amorphous materials and thus the attempt to correlate the molecular assembly and the optical spectra, for an amorphous species, is not obvious. In

this general context the present contribution underlines the spectroscopic behaviour of ruthenium phthalocyanine dimer $(\text{PcRu})_2$, both in solution and in the solid phase. Indeed $(\text{PcRu})_2$ was the object of a previous contribution of ours⁸ in which we presented the structural, electrical and magnetic features of this compound and its reactivity towards oxygen, all properties being connected with the Ru–Ru double bond and the dimeric nature of the compound itself. In the light of the amorphous nature of the compound, the structural investigation was carried on using the LAXS (Large Angle X-ray scattering) and EXAFS (Extended X-ray Absorption Fine Structure)⁹ techniques. In a more recent paper we extended the former technique to the $(\text{PcRu})_2$ amorphous films so confirming that, when deposited as a film by vacuum evaporation, the material maintains its molecular dimeric arrangement unchanged.¹⁰ In this work an accurate spectroscopic characterisation of the material, in solution, as a powder and as evaporated films, by UV-Visible (UV-Vis) and infrared (IR) spectroscopy is presented. The obtained data are discussed as functions of the different molecular arrangements in solution and in the solid phase. The surface chemical composition and depth profiling were investigated by X-ray photoemission spectroscopy (XPS) which is widely used for the analysis of the first monolayers of the surface. EXAFS studies, aimed at defining the structural features of films, are also presented.

Experimental

$(\text{PcRu})_2$ was synthesized as already described¹¹ and the compound purity was checked by elemental analysis (calc. for $(\text{C}_{32}\text{H}_{16}\text{N}_8\text{Ru})_2$ C, 62.64; N, 18.26; H, 2.63; found C, 62.26; N, 18.23; H, 2.53%). Films were prepared by evaporation from

a molybdenum boat on an Edwards A306 coater at $\approx 350^\circ\text{C}$ and 10^{-6} Torr, the substrate being at room temperature.

Different substrates were used for different analyses as follows: for UV-Vis investigation optical grade quartz plates, for IR spectroscopy CsI windows, for XPS and EXAFS analysis glass plates. Unless otherwise specified, the film thicknesses, monitored by an Edwards FTM5 Crystal Balance Monitor (density: 1.6), ranged from 80 to 100 nm.

UV-Vis spectra were recorded on a Cary 5 spectrophotometer and IR spectra on a Perkin Elmer 16Pc FTIR.

EXAFS spectra were measured at the ruthenium K-edge (22116 eV) at the GILDA Italian CRG beamline of the European Synchrotron Radiation Facility in Grenoble (France). The typical ring current was about 125 mA and a flux of the order of 10^9 photons s^{-1} was available during measurements.

The EXAFS experiments were performed in the dark at liquid nitrogen temperature by recording the fluorescence signal, collected by a plastic detector capped with a 100 μm thick aluminium foil, from phthalocyanine films. Each spectrum spans 1000 eV above the edge and the k -spacing was kept constant in order to collect at least 500 data points.

In order to test the reliability of the measurements a preparation of the ruthenium phthalocyanine compound was deposited as a film by sublimation on glass substrates. The consistency between independent measurements was tested and found to be better than 3% averaged on all the structural information. EXAFS analysis was performed with the EXCURV92¹² program, which is very appropriate when aromatic rings are involved. In fact it is possible to consider a ring as a single unit by using a limited number of parameters and to describe the ligand up to roughly 5 Å from the ruthenium centre.

The same parameters as used for the bulk material in a previous elaboration⁹ were used in the present paper to fit the experimental data. The four symmetric rings in the ruthenium plane were described as being related by rotation around the C_4 axis perpendicular to the molecular plane whereas the ruthenium-bonded α -nitrogens are at fixed distances from the β -nitrogens and the γ -carbons. When the distance between the central absorbing atom and the first shell ligand is varied, the whole ring, as a single highly correlated unit, is accordingly shifted. Both the intra- and inter-rings correlations were taken into account in order to maintain the overall structure of the phthalocyanine molecule. The fitting procedure took into account the predictable displacement of the ruthenium absorbing atom from the N_4 inner plane and the possible deviation of the phthalocyanine molecule from planarity, by varying the polar coordinates. This choice makes it possible to limit the number of parameters necessary to describe the ring. In our case the number of independent parameters for the ring atoms equals six. All the rings are considered correlated by symmetry operation. The co-ordination numbers were kept constant in the refinement procedure and the numbers of independent parameters relative to the overall structure of the dimeric $(\text{RuPc})_2$ molecule are: six from the rings, two from external bridging nitrogens, two from the bonded ruthenium and four from the rings of the second macrocycle unit. The independent parameters total fourteen, which is compatible with the number of independent experimental points available. The data interval chosen to perform the Fourier transform was suitable to remove the most of the high energy noise. More confidence in the fit was achieved through the total fitting procedure where all the shells up to 5 Å are calculated together, so minimizing the effects of side lobes due to the Fourier terminations. The Fast Curved Wave Theory, which includes multiple scattering (MS) processes, was used to evaluate the contributions from the highly symmetric four pyrrolic rings around the metal ion up to the β carbon atoms. The minimum number of shells necessary to take into account the

contribution of the multiple scattering from the atoms within the ruthenium plane was computed. In all refinements the co-ordination numbers for all the considered shells and the geometric description of the pyrrolic rings were kept fixed and never refined, using a maximum number of five independent shells. In the present case the number of independent points $N = [(dkdr/\pi)] + 2$ exceeds the maximum of fourteen parameters used for the dimeric molecule.

The surface chemical composition of film samples was studied by XPS, in an ultrahigh vacuum (UHV) system with a base pressure $P = 10^{-7}$ Pa. The UHV chamber was equipped with a VG ESCALAB MKII spectrometer, a standard Al $K\alpha$ excitation source ($h\nu = 1486.6$ eV) and a five-channeltron detection system. Samples were positioned at the electron take-off angle normal to the surface with respect to the hemispherical analyser set to a constant pass energy ($E_p = 20$ eV). The binding energy (BE) scale was calibrated by measuring reference C 1s peaks (BE = 285.0 eV) from the surface contamination. The accuracy of the measured BE was ± 0.2 eV. Depth profiles of samples, positioned under an Au mask (4×4 mm²), were acquired by using selected-area XPS (SAXPS) combined with cycling Ar⁺ sputtering (2 keV). In the SAXPS mode, photoelectrons were collected from a 1 mm diameter area on the sample surface.

A non-linear least-squares curve-fitting routine was used to analyse the XPS spectra, by separating elemental species in different oxidation states. The relative chemical element concentrations were calculated by a standard quantification routine, including Wagner's energy dependence of attenuation length¹³ and a standard set of VG Escalab sensitivity factors. The XPS data were collected and processed by using a Digital Micro-PDP computer system and VG S5250 software.

Results and discussion

XPS analysis

Several samples of $(\text{RuPc})_2$ films with different thicknesses were analysed by XPS spectroscopy. The surface composition results and the depth profile analyses are very similar for all the investigated samples. The surface qualitative and quantitative chemical composition and depth profiling of a 70 nm thick $(\text{RuPc})_2$ film are reported.

The binding energy (BE) values of the main XPS peaks (Ru 3d_{5/2} and N 1s) and the relative chemical composition of the $(\text{RuPc})_2$ film and reference samples of $(\text{PcRu})_2$ and ruthenoxane derivative $\text{HO}[(\text{Pc})\text{RuO}]_n\text{H}$ powders are reported in Table 1. The BE values are characteristic of the elements in their formal oxidation state as confirmed by literature data.^{14,15} The analysis of the XPS spectrum in the Ru 3d + C 1s region (279–291 eV) was performed by a curve-fitting procedure in order to distinguish and separate ruthenium and carbon species in different chemical environments. The XPS spectra of the $(\text{RuPc})_2$ powder samples show a component at $\text{BE} = 281.5 \pm 0.2$ eV, attributable to Ru(II) in the $[\text{RuN}_4]$ chromophore group of $(\text{RuPc})_2$,¹⁴ and another component at $\text{BE} = 282.6 \pm 0.2$ eV, attributable to ruthenium species in the $[\text{RuN}_y\text{O}_x]$ chromophore group¹⁵ (see Table 1).

In accordance with the results of the curve-fitting, the Ru 3d peak is dominated by a major component at $\text{BE} = 281.5 \pm 0.2$ eV, attributable to Ru(II) in the $[\text{RuN}_4]$ chromophore group of $(\text{RuPc})_2$. Another component at $\text{BE} = 282.6 \pm 0.2$ eV is evidenced by the curve-fitting procedure. This is assigned to ruthenium species in the $[\text{RuN}_y\text{O}_x]$ chromophore group, as already reported¹⁵ and found in the reference ruthenoxane ($\text{HO}[(\text{Pc})\text{RuO}]_n\text{H}$) powder sample (see Table 1). It is very difficult to assign a precise oxidation state to ruthenium, as literature data on Ru(III) and Ru(IV) species in an analogous chemical environment are lacking. Therefore, this component is attributed to ruthenium species with higher

Table 1 XPS quantitative analysis. Binding energy (BE) values of Ru 3d_{5/2} and N 1s peaks, relative chemical composition (atomic ratio) of the (RuPc)₂ film. Reference samples of (RuPc)₂ and ruthenoxane HO[(Pc)RuO]_nH powders are reported. Elemental concentrations are normalised to the Ru 3d_{5/2} peak at BE=281.7±0.2 eV, assigned to (RuPc)₂

Sample		Ru 3d _{5/2}		N 1s	Ru/N
(RuPc) ₂ film	BE/eV	281.5	282.4	399.8	
	Atomic ratio	1.00	0.16	7.70	1/8
(RuPc) ₂ powder	BE/eV	281.7	282.8	399.6	
	Atomic ratio	1.00	0.21	8.71	1/9
HO[(Pc)RuO] _n H	BE/eV	281.9	282.8	399.5	
	Atomic ratio	1.00	1.06	9.02	1/9

charge density as a result of the XPS analysis of suitable reference compounds, *i.e.* (RuPc)₂ powder and ruthenoxane in which ruthenium species in different chemical environments, [RuN₄] and [RuN_yO_x], are present.

No evidence of a ruthenium metallic component at BE=280.1±0.2 eV¹⁴ can be found in the XPS spectrum of the film, at variance with other literature reports.¹⁶

The analysis of XPS data for the (RuPc)₂ film is in good agreement with that for the powder compounds taken as reference, as shown in Table 1. The elemental concentrations, expressed as the Ru/N atomic ratio, are normalised to the Ru 3d_{5/2} peak at BE=281.5±0.2 eV. The component relative concentration at BE=282.6±0.2 eV, assigned to ruthenium species in the [RuN_yO_x] chromophore group, significantly increases in the ruthenoxane powder sample (see Table 1).

For all the investigated samples the curve-fitting of the C 1s peak consists of three components, at BE=285.0±0.2, 286.5±0.2 and 288.0±0.2 eV, attributable to an aromatic ring carbon, an alkoxy [-CH₂O_x] species and an oxidised [-COO⁻] group, respectively, as already reported.^{14,17} The N 1s photoelectron peak is located at BE=399.5±0.2 eV in all the XPS spectra for the samples, in good agreement with the value reported for nitrogen in the metal-coordinated phthalocyanine macrocycle.¹⁸

The qualitative and quantitative chemical composition of the (RuPc)₂ film was also investigated throughout the thickness by depth profile analysis, which confirmed a 70 nm thickness for the film. The three-dimensional qualitative profiles of the Ru 3d_{5/2} and C 1s region (270–300 eV) as a function of the sputtering time are shown in Fig. 1a. The quantitative profile of the (RuPc)₂ film as a function of the film depth is reported in Fig. 1b. The value of the Ru/N atomic ratio is 1/8 on the surface, as reported in Table 1, and it remains almost constant throughout the thickness (70 nm) of the film, up to the sharp drop corresponding to the film/substrate interface. These results confirm the homogeneity and the stability of the (RuPc)₂ film composition all throughout the thickness and the formation of a sharp interface, with no chemical bonds between the film and the substrate.

EXAFS analysis

EXAFS investigation is a very useful tool to obtain accurate structural information for samples which do not possess long-range order, and this technique was previously used for the study of bulk (RuPc)₂;⁹ this paper reports the results obtained for the analogous compound deposited as a film. Four independent data analyses were carried out on two samples (I, II) of ruthenium phthalocyanine films originating from the same chemical preparation. Since these two samples were prepared at constant substrate temperature and variable distances between the substrate and the source material, they only differ in the deposition rate. The collected data were independently recorded and fitted in order to evaluate the fitting sensitivity to reproduce the overall structural data for the system. The best fits are presented in Figs. 2–4, and values are reported in Table 2 where the distances and the Debye–Waller type parameters used to fit data for both depositions are

listed. The first reasonable fit for film I was obtained with the same parameters and values as already reported for the bulk sample. The first deduction one can reach is the evidence that the film presents a dimeric structure which is not destroyed by vacuum deposition. The bond distances are very close to those found for the powder sample except for two contributions. The first contribution is related to four inner nitrogens belonging to the second macrocycle (ring A' still inside the same dimer) found at a distance of 3.62 Å instead of 3.34 Å. The second one is related to the distance ruthenium–ruthenium of the second dimeric unit which in the film is found to be 4.51 Å instead of 4.46 Å as reported for the powder. For the second sample (II) examined, only slightly longer distances are used to fit data, with the considerable exception of the intradimeric distance Ru–Ru which is less than 0.025 Å. Since the error in the first shell is far smaller than the differences found, this result gives evidence that the two ruthenium atoms are actually closer to each other, and each ruthenium atom is located out of the N₄ plane at a longer distance also in accordance with what was found for the atoms in α, β and γ positions.

The most evident differences between bulk and films are the longer distances of the absorbing atom from the nitrogens of

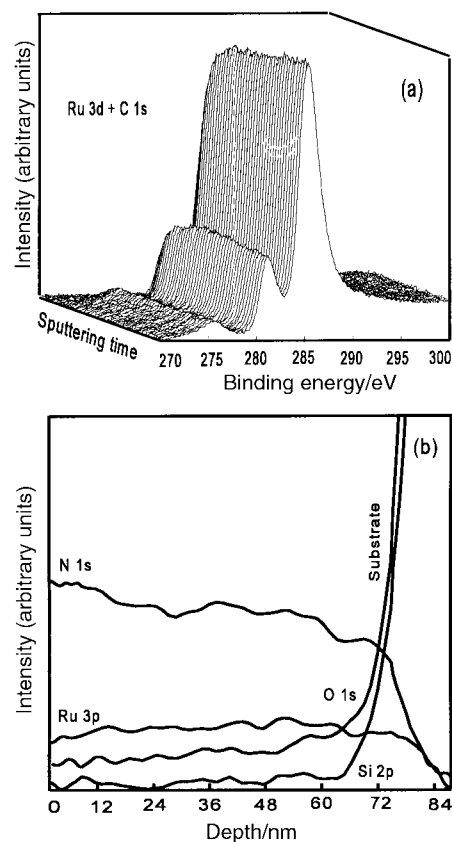


Fig. 1 XPS depth profile of the (RuPc)₂ film. In (a) the three-dimensional qualitative profile in the Ru 3d and C 1s region (270–300 eV) is reported as a function of the sputtering time. In (b) the quantitative profile is plotted as function of the depth.

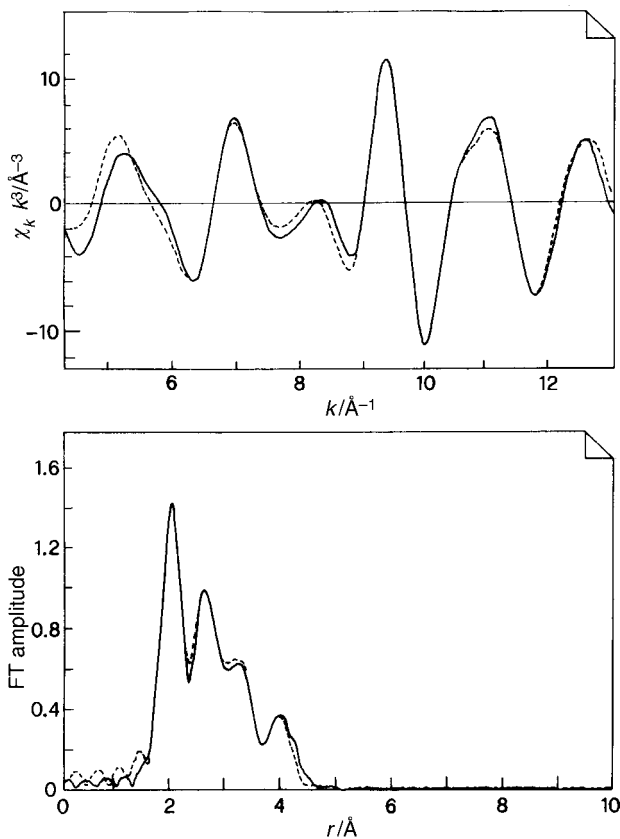


Fig. 2 Above: observed (solid line) and calculated (dotted line) $\chi_k k^3$; below: respective Fourier transform for sample I.

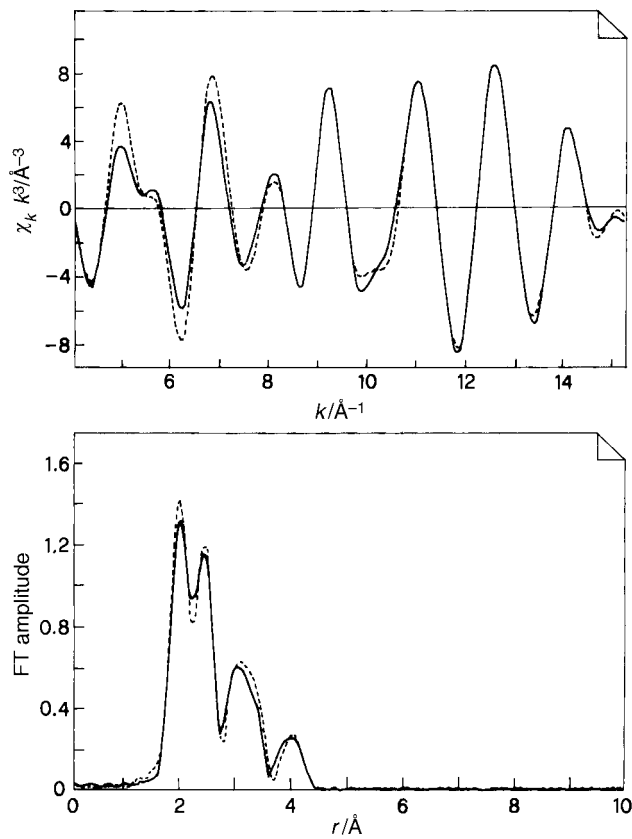


Fig. 4 Above: observed (solid line) and calculated (dotted line) $\chi_k k^3$; below: respective Fourier transform for sample I after ageing.

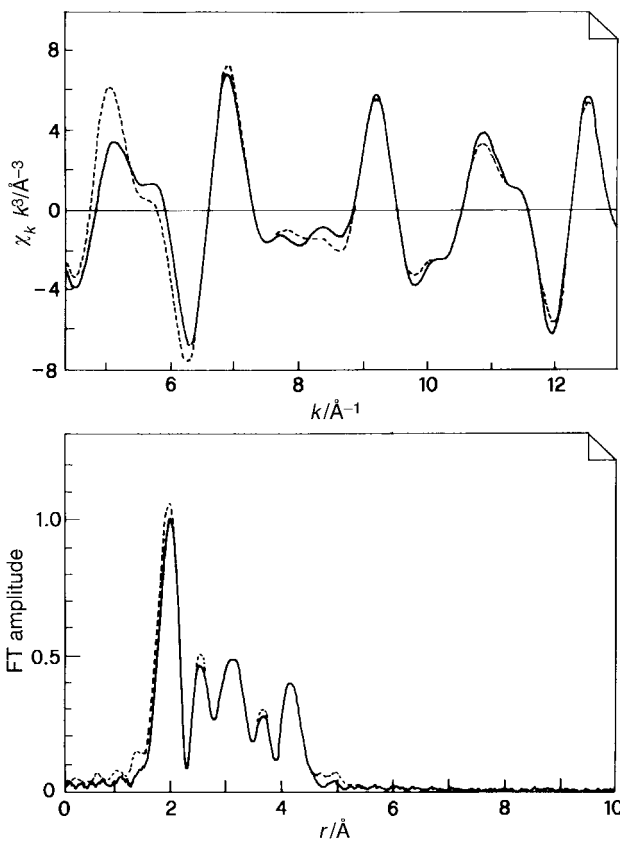


Fig. 3 Above: observed (solid line) and calculated (dotted line) $\chi_k k^3$; below: respective Fourier transform for sample II.

ring A', up to 0.5 Å, (see sample II) and the longer Ru–Ru interdimer distance (0.05 Å). Since the interdimeric Ru–Ru distance increase is less than the Ru–N increase (A' ring), one can deduce that the macrocycles are more distorted towards a domed conformation, but since the average distance between two dimers in the stack is not changed significantly we believe that this is indeed the reason for this extended deformation.

One third measurement set was recorded on sample I after a couple of months ageing and the obtained data are almost indistinguishable from those shown for sample II. The observed slight differences can reasonably be attributed to the effect of the temperature (liquid nitrogen) to which the sample was subjected during the previous measurements.

Further interesting structural data were obtained after annealing the aged sample I at 150 °C for 1 hour. Results of the fit for the extracted EXAFS spectrum and related Fourier transform are reported in Fig. 5. The only remarkable difference found with its precursor (aged sample) concerns the Ru–Ru intradimeric distance as shown in Table 3. The best fit index was indeed achieved without any contribution of the far ruthenium atom belonging to the next molecule, which in the untreated film was at 4.52 Å of the side lobe. Both the fit index and the residuals between the experimental and calculated EXAFS spectra are excellent, but it is possible, under the Joyner significance test,¹⁹ to add a new shell taking into account the contribution from the distant ruthenium. Two more fits showing a very similar fit index and a better residual were obtained. They give Ru–Ru distances at 4.48 Å (refinement of the distance in sample I as reported in Table 2) and at 4.66 Å (refinement obtained for the fluctuation of the distances). In both fits the Debye–Waller type factors are extremely high for these contributions, while the rest of the distances and disorder factors are not affected by the new added shell. This indicates a disordered situation; it is very likely that the thermal treatment modifies the arrangement between the dimeric units.

Table 2 EXAFS determined interatomic distances (r) in $(\text{RuPc})_2$ films: sample **I**, fit index (F.I.) 2.06; residual (R) 19.25; sample **II**, F.I. 1.6184; R 22.74, and sample **II** after ageing, F.I. 1.5811; R 16.56. $\Delta E_0 = 15.08$ eV. n = coordination number; σ = Debye-Waller type factor; A, A' = Pc rings of the dimeric unit; B = Pc ring of the closest dimeric unit

	n	Sample I		Sample II		Sample I after ageing	
		$r/\text{\AA}$	$\sigma/\text{\AA}$	$r/\text{\AA}$	$\sigma/\text{\AA}$	$r/\text{\AA}$	$\sigma/\text{\AA}$
Ru-N(A)	4	1.978 ± 0.01	0.032	1.999 ± 0.01	0.035	1.999 ± 0.01	0.032
Ru-Ru(A')	1	2.401 ± 0.01	0.039	2.375 ± 0.01	0.065	2.383 ± 0.01	0.039
Ru-C(A)	4	2.967 ± 0.01	0.045	3.027 ± 0.01	0.016	3.027 ± 0.01	0.012
Ru-C(A)	4	2.956 ± 0.01	0.045	3.015 ± 0.01	0.072	3.015 ± 0.01	0.000
Ru-N(A)	4	3.246 ± 0.01	0.035	3.283 ± 0.01	0.000	3.229 ± 0.01	0.080
Ru-N(A')	4	3.623 ± 0.01	0.032	3.821 ± 0.01	0.060	3.367 ± 0.01	0.032
Ru-Ru(B)	1	4.511 ± 0.01	0.150	4.518 ± 0.01	0.060	4.523 ± 0.01	0.011
Ru-C(A')	4	3.949 ± 0.01	0.000	4.051 ± 0.01	0.016	4.032 ± 0.01	0.045
Ru-C(A')	4	3.883 ± 0.01	0.032	3.986 ± 0.01	0.000	4.008 ± 0.01	0.005

Table 3 EXAFS determined interatomic distances (r) in RuPc_2 film sample **II** after ageing and temperature treatment. Three fit results are reported in three columns; $\Delta E_0 = 15.08$ eV. n = coordination number; σ = Debye-Waller type factor; A, A' = Pc rings of the dimeric unit; B = Pc ring of the closest dimeric unit

	n	F.I. 1.61, R 18.48		F.I. 1.908, R 17.30		F.I. 1.71, R 16.02	
		$r/\text{\AA}$	$\sigma/\text{\AA}$	$r/\text{\AA}$	$\sigma/\text{\AA}$	$r/\text{\AA}$	$\sigma/\text{\AA}$
Ru-N(A)	4	1.986 ± 0.01	0.032	1.997 ± 0.01	0.027	1.998 ± 0.01	0.027
Ru-Ru(A')	1	2.383 ± 0.01	0.035	2.381 ± 0.01	0.032	2.381 ± 0.01	0.032
Ru-C(A)	4	3.031 ± 0.01	0.055	3.019 ± 0.01	0.090	3.016 ± 0.01	0.099
Ru-C(A)	4	3.022 ± 0.01	0.052	3.008 ± 0.01	0.000	3.005 ± 0.01	0.000
Ru-N(A)	4	3.278 ± 0.01	0.016	3.241 ± 0.01	0.060	3.233 ± 0.01	0.003
Ru-N(A')	4	3.384 ± 0.01	0.052	3.347 ± 0.01	0.039	3.349 ± 0.01	0.027
Ru-Ru(B)	1	—	—	4.482 ± 0.01	0.110	4.659 ± 0.01	0.105
Ru-C(A')	4	4.004 ± 0.01	0.035	4.013 ± 0.01	0.047	4.011 ± 0.01	0.047
Ru-C(A')	4	3.874 ± 0.01	0.087	3.994 ± 0.01	0.005	3.992 ± 0.01	0.050

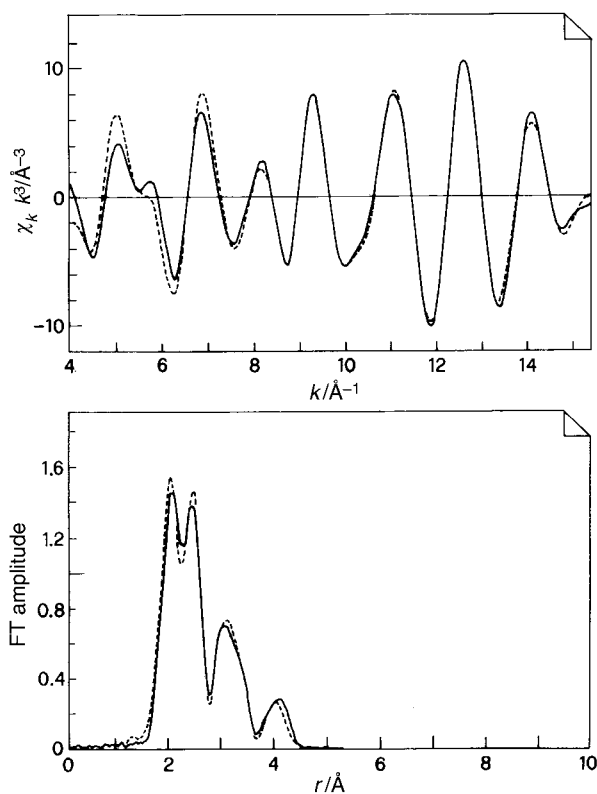


Fig. 5 Above: observed (solid line) and calculated (dotted line) $\chi_k k^3$; below: respective Fourier transform for sample **I** after ageing and temperature treatment.

The fitting procedure was indeed kept identical for all the discussed data sets, especially in order to test the reproducibility and the confidence of the fits. In this respect we noticed a very sensitive region of the spectrum, around 3.5 Å. Nitrogens of the second ring (A') are present at this distance from the absorbing ruthenium and we believe that this large sensitivity of these atoms to any small change in distance is strictly connected with the displacement of the ruthenium atom out of the N_4 plane.

In conclusion EXAFS data show, on the one hand, that the ruthenium phthalocyanine is a very stable dimer and, on the other hand, that the molecule has a relative flexibility in displacing the ruthenium out of the plane and in deforming the macrocycles subject to different factors such as deposition conditions or thermal treatments.

Infrared spectra

It is well known that different polymorphic organisations of phthalocyanines also show different IR absorbance patterns which can be useful in identifying and characterizing a particular form or dimorphic transition. In particular, in the range between 800–700 cm^{-1} the out-of-plane C–H bending vibrations are expected. In fact, due to the sensitivity of these vibrations to the molecular packing, the major differences reported so far for both metallated phthalocyanines and the free ligand of different polymorphic structures were discovered in this range.⁶ In Fig. 6 we reported the IR spectra in KBr of $(\text{RuPc})_2$ as the bulk product (a) and as an evaporated film (b). As can be seen, the spectra are very similar in the shown range, but in the above mentioned region some differences can be noticed: the three band system is constituted in (a) by well defined bands at 726, 754, 770 cm^{-1} while in (b) the first one is centred at 728 cm^{-1} with a pronounced shoulder at 734 cm^{-1} and the third one is centred at 778 cm^{-1} with a shoulder at 766 cm^{-1} . In the neighbourhood of 850 cm^{-1} , although the

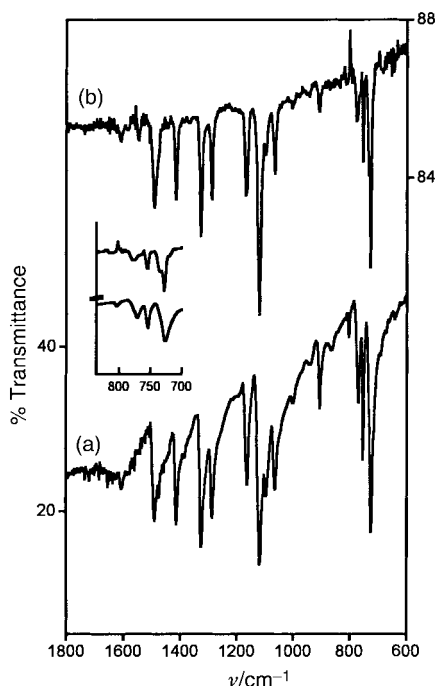


Fig. 6 IR spectra of $(\text{RuPc})_2$: a) bulk in KBr, b) film on CsI window; inset: enlargement of the $850\text{--}700\text{ cm}^{-1}$ range.

intensity of the peaks for both the bulk and film spectra was very low, one can notice the disappearance, in the film spectrum, of the peak at 866 cm^{-1} which is also considered to be sensitive to the molecular packing. These slight differences could be attributed to different molecular assembling in the bulk and in the film. These small differences are similar to the differences attributed to α and β forms in Sharp *et al.*²⁰ The recent findings reported by the authors,⁹ which assign a higher number of stacked dimers in the film compared with the bulk, could suggest the explanation of these IR differences together with the differences in optical spectra reported below.

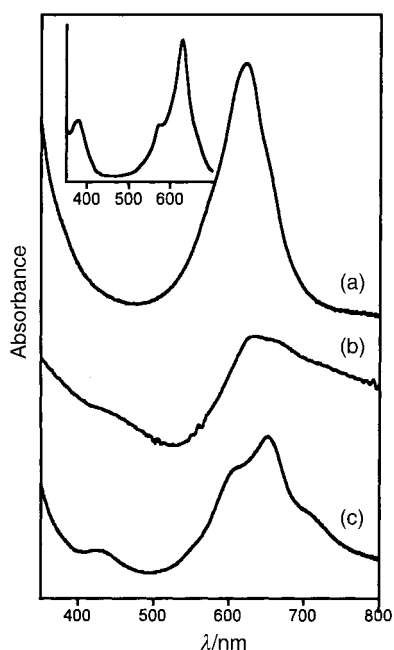


Fig. 7 Visible spectra of $(\text{RuPc})_2$: a) dissolved in 1-chloronaphthalene, b) in the solid state as Nujol mull, c) film on quartz plate; inset: spectrum of $\text{PcRu}(\text{Py})_2$ in 1-chloronaphthalene.

Visible spectra

In Fig. 7 the spectra of $(\text{PcRu})_2$ in solution and as the solid phase are shown. Spectrum (a) is that of $(\text{RuPc})_2$ in 1-chloronaphthalene while the inset spectrum is associated with $\text{RuPc}(\text{py})_2$ in the same solvent. For the former spectrum, the solution was prepared and the spectrum itself was recorded in a strictly inert atmosphere (N_2) in consideration of the high reactivity towards oxygen of the dimeric form when dissolved in a weak or non-coordinating solvent.⁸ This circumstance makes it hard to assign the UV-Vis spectrum to the dimeric species in various solvents. On the other hand, it is widely known that this same species, when dissolved in coordinating solvents (L), originates the adduct monomeric form $\text{RuPc}(\text{L})_2$ whose visible spectra have been reported in the literature.²¹ Nevertheless, despite the mentioned difficulty, in consideration of the strict experimental conditions we adopted, we can reasonably assume that the obtained spectrum is attributable to the dimeric form $(\text{RuPc})_2$.

It is well known that the metallophthalocyanines belong to the point group D_{4h} ; their electronic structure was described by Gouterman²² and in depth by Stillmann and Nyokong.²¹ In detail, the HOMO (Highest Occupied Molecular Orbital) level is $1a_{1u}(\pi)$, the next low lying filled orbital is $1a_{2u}(\pi)$, the LUMO (Lowest Unoccupied Molecular Orbital) orbital is $1e_g(\pi^*)$ and the next one is $1b_{1u}(\pi^*)$. The transitions from the two upper filled π orbitals to $1e_g(\pi^*)$ yield the so-called Q (near $600\text{--}750\text{ nm}$) and Soret (or B) (near $300\text{--}450\text{ nm}$) $\pi\text{--}\pi^*$ transitions.

In our case (Table 4) the Q band of the solution spectrum (Fig. 1a) shows a maximum at 623 nm and two very slight shoulders, one at higher and one at lower energy. The solid phase spectrum in Nujol (Fig. 7b) is remarkably less resolved, the maximum is broad, asymmetric and shifted towards lower energy (635 nm); a slight absorbance centred at 430 nm is also present. In the spectrum of the evaporated film (Fig. 7c) the maximum of the Q band is further red-shifted to 651 nm while a pronounced shoulder at 608 nm and a less evident one at 720 nm can be observed. A marked shifting towards lower energy is, on the whole, observed for $(\text{RuPc})_2$ spectra when moving from solution to film *via* a solid phase step.

The interpretation of solid state spectra of phthalocyanines is commonly performed by the theory of exciton coupling.^{3,7} In a very simplified way we can say that this theory is based on the interaction between adjacent molecules (dimers) although it was also extended to molecules in infinite stacks.²³ The appearance of a broader Q absorption shifted to the blue in the solid state spectrum is attributed to near or full cofacial alignment of two or more phthalocyanine molecules. This is, in fact, a characteristic feature of the H_2Pc ,²⁴ MPc ²⁰ spectra, but also of covalently bonded dimers or polymers such as μ -oxo bridged $\text{M}(\text{IV})\text{Pc}$.^{25,26} When the exciton interaction concerns two non-cofacial but edge-to-edge arranged phthalocyanines, theory anticipates a red-shifted Q band. This is the case for the β and X phases of H_2Pc ²⁰ and MPc ,²⁴ but also for the triclinic phases of PbPc ²⁷ and OTiPc .²⁸ Very often the solid state spectra show a less or more extended splitting of the peaks

Table 4 Q-Band wavelengths of selected metallophthalocyanines according to literature data and this work

	Nujol			Ref.
	Solution	mull	Film	
$(\text{PcRu})_2$	623	635	651	This work
PcFe	691			21
PcCu	678		625–694 (α), 645–720 (β)	24
PcSn	690			26
Pc_2Sn	625			26
$\text{PcSi}(\text{OH})_2$	671			25
$(\text{PcSiO})_2$	630			30
$(\text{PcSiO})_n$		625		25

(Davydov splitting) also predicted by theory. In fact dimers, which are in a tilted arrangement with one another, will have a spectrum with a split Q band which is both red and blue shifted.

As can be observed, the spectra features of (RuPc)₂ are quite singular; the Q band of the isolated dimer in solution is in fact at 623 nm. Unfortunately no correlation can be made with the corresponding monomeric form as it does not exist. Nevertheless, the principal peak falls at higher energy (about 30 nm) than the absorbance of other monomeric phthalocyanines in the same solvent (Table 4). This first evidence can be perfectly explained by the exciton coupling theory. As a matter of fact the two macrocycles of the molecule bridged by a Ru=Ru double bond are a cofacial arranged dimer (assembly) for which, according to theory, only the transition to the higher energy levels of the excited state is allowed. This can also be found in the case of the porphyrin analogous ruthenium octaethylporphyrin (RuOEP)₂.²⁹ A similar behaviour was observed for the single unit SiPc(OH)₂ and its corresponding oligomeric forms in solution.³⁰

The previous structural findings on (RuPc)₂ powders and films⁸⁻¹⁰ demonstrated that in the solid state the dimeric molecules are assembled in stacks of about six dimers (superimposed in the direction parallel to Ru–Ru bonds), which become ten when the material is deposited as a film. The ruthenium atom within the dimer is 0.41 Å out of the inner N₄ plane of the macrocycle ring, the two phthalocyanine rings within the molecule are not perfectly planar and assume a domed conformation with each ring being slightly bent outward from the inner N₄ plane (0.15 Å), the macrocycles assume a staggered position with a rotation angle of ca. 45° staggering and eclipsing alternately along the stacking direction. Furthermore, side-by-side arranged chains at a distance of 15.9 Å were found. Owing to the amorphous nature of both powder and film, it has not so far been possible to assign the molecular symmetry to this molecule (although, for strict analogy with the (RuOEP)₂ molecule, it is likely to approach D_{4d} symmetry) and for this one-dimensional cofacial stack it is not possible to find any analogy with a known polymorphic form. On the basis of the gathered information it would be reasonable to expect a blue shift of the Q band in the solid state spectra, but this was not the case. In fact a red shift of the Q band is observed for the transmission spectrum of the material in Nujol mull and, to a more considerable extent, for the spectrum of its corresponding thin film on a quartz substrate. An attempt to apply the semi-empirical modification of exciton coupling model according to Fujiki *et al.*²³ did not yield any reasonable result.

A different point of view about the optical behaviour of solid state MPcs was presented by Mizuguchi *et al.*³¹ who explained the red shift of the Q band of non-planar MPcs with the influence of molecular distortion on the approach of ring moieties due to π – π interactions along the stacks. As mentioned above, this kind of behaviour is reported for Pcs in β and X phases and for triclinic asymmetric derivatives. The case under examination, concerning two parallel chains at a distance of 15.9 Å built up by dimeric ruthenium phthalocyanine molecules at an average inter-unit distance of 3.36 Å, can be considered as a cofacially assembled system with a significant π – π interaction and a remarkable molecular distortion due to the domed conformation of the rings (see also EXAFS results above). In this case it is not easy to predict the optical behaviour in the absence of theoretical calculations, but it seems right to explain our results in terms of interplanar π – π interactions and molecular distortion which are the two outstanding aspects. The very small distance between the concave and convex macrocycles within the same dimer, together with the small distance between the dimers in the stacks, yields a strong π – π contact between superimposed macrocycles along the stacking axis so lowering the transition energy between e_g–a_{1u} orbitals. This feature could also be

responsible for the difference between the absorption of the Q band in the film and the bulk spectra. In fact, as we already mentioned, the number of superimposed dimers is found to be ten for the film vs. six for the bulk and therefore the interaction is likely to be enhanced in the film. On the other hand it is undoubted that also the conductivity of (PcRu)₂ is considered anomalous, being 10⁻⁵ Ω⁻¹ cm⁻¹ (pressed pellet value), 5 orders of magnitude higher than other undoped MPcs. Also this feature has been considered as a result of the very strong interaction of π – π planes.⁸

All the above considerations prompt us to suggest that the intermolecular interactions are the predominant factor to be taken into account in explaining the electronic spectra in the solid state. In fact the tendency of the dimeric molecules to arrange themselves in a one-dimensional stack with a very short distance between planes is likely to be attributed to a bonding interaction existing along the stack. This interaction could make this kind of packing thermodynamically favourable. Therefore the driving force for the assembly may also be considered able to tune the molecular deformation in order to adjust the units in the stack, as demonstrated by EXAFS analysis.

Optical spectra also recorded for films thermally treated at 150 °C did not show any shift of the Q band. They only appeared more broadened than the corresponding untreated film spectra according to the structural information obtained by a previous LAXS investigation⁹ and confirmed by the EXAFS studies here reported.

Conclusions

The optical absorption spectra of (RuPc)₂ have been recorded in solution, as a powder and as a film. The data, supported by EXAFS investigations, allow us to draw some interesting conclusions as follows. The dimeric molecule of (RuPc)₂ itself, in the solid phase, is heavily distorted, the phthalocyanine macrocycles are bent outward from the inner N₄ plane assuming a concave and convex form within the same molecule in a staggered conformation. The appearance of the optical spectrum and the lower energy transition observed in solution compared with other metallophthalocyanines is attributed to the cofacial arrangement of two macrocycles as predicted by the coupling exciton theory. Conversely, the red shifted absorption observed when moving from solution to the solid state is related to the strong π – π interaction due to the contacts along the molecular stack. Molecular distortions and π – π interplanar contacts are closely linked, but we suggest that in the solid phase the packing made up of superimposed dimeric molecules is promoted by a large attitude of the dimeric units to approach each other in a way suitable to delocalise the electronic clouds so stabilising the supramolecular arrangement.

References

- 1 *Phthalocyanines: Properties and Applications*, ed. C. C. Leznoff and A. B. P. Lever, vol. 1–4, VCH, Weinheim, 1989–1996.
- 2 F. H. Moser and A. L. Thomas, *The Phthalocyanines*, vol. I, VCH, New York, 1983.
- 3 M. J. Cook, in *Spectroscopy of New Materials*, ed. R. J. H. Clark and R. E. Hester, CRC Press, Boca Raton, FL, 1993, p. 87 and references therein.
- 4 E. A. Lucia and F. D. Verderame, *J. Chem. Phys.*, 1968, **48**, 2674.
- 5 B. R. Hollebome and M. J. Stillman, *J. Chem. Soc., Faraday Trans. 2*, 1978, **74**, 2107.
- 6 B. Stymne, F. X. Sauvage and G. Wettermark, *Spectrochim. Acta*, 1979, **35A**, 1195.
- 7 M. Kasha, H. R. Rows and M. A. El-Bayoumi, *Pure Appl. Chem.*, 1965, **11**, 371.
- 8 A. Capobianchi, A. M. Paoletti, G. Pennesi, G. Rossi, R. Caminiti and C. Ercolani, *Inorg. Chem.*, 1994, **33**, 4635.

- 9 L. Alagna, A. Capobianchi, P. Marovino, A. M. Paoletti, G. Pennesi, T. Prosperi and G. Rossi, *Inorg. Chem.*, 1999, **38**, 3688.
- 10 R. Caminiti, A. Capobianchi, P. Marovino, G. Pennesi, A. M. Paoletti and G. Rossi, *Thin Solid Films*, in press.
- 11 M. Hanack, S. Osio-Barcina and E. Witke, *Synthesis*, 1992, 211.
- 12 S. J. Gurman, N. Binsted and I. Ross, *J. Phys. C*, 1986, **19**, 1845.
- 13 C. D. Wagner, L. E. Davis and W. M. Riggs, *Surf. Interface Anal.*, 1986, **2**, 53.
- 14 J. F. Moulder, W. F. Stickle, P. E. Sobol and K. D. Bomben, in *Handbook of X-Ray Photoelectron Spectroscopy*, ed. J. Chastain and R. C. King Jr., Electronics Inc., Eden Prairie, MN, USA, 1995.
- 15 A. Capobianchi, A. M. Paoletti, G. Pennesi, G. Rossi, R. Caminiti, C. Sadun and C. Ercolani, *Inorg. Chem.*, 1996, **35**, 4643.
- 16 D. Smeißer, J. Pohmer, M. Hanack and W. Göpel, *Synth. Met.*, 1993, **61**, 115.
- 17 C. Battistoni, M. P. Casaletto, G. M. Ingo, S. Kaciulis, G. Mattogno and L. Pandolfi, *Surf. Interface Anal.*, 2000, **29**, 773.
- 18 Y. Niwa, H. Kobayashi and T. Tsuchiya, *J. Chem. Phys.*, 1974, **60**, 799.
- 19 R. W. Joyner, K. J. Martin and P. Meehan, *J. Phys. C: Solid State Phys.*, 1987, **20**, 4005.
- 20 J. H. Sharp and M. Lardon, *J. Phys. Chem.*, 1968, **72**, 3230.
- 21 M. J. Stillmann and T. Nyokong, in *Phthalocyanines: Properties and Applications*, ed. C. C. Leznoff and A. B. P. Lever, vol. 1, VCH, Weinheim, 1989, p. 135 and references therein.
- 22 M. Gouterman, in *The Porphyrins*, vol. 3, ed. D. Dolphin, Academic Press, New York, p. 1.
- 23 M. Fujiki, H. Tabei and T. Kurihara, *J. Phys. Chem.*, 1988, **92**, 1281.
- 24 J. H. Sharp and M. Abkowitz, *J. Phys. Chem.*, 1973, **77**, 477.
- 25 C. W. Dirk, T. Inabe, K. F. Schoch Jr and T. J. Marks, *J. Am. Chem. Soc.*, 1983, **105**, 1539.
- 26 O. Ohno, N. Oshikawa, H. Matsuzawa, Y. Kaizu and H. Kobayashi, *J. Phys. Chem.*, 1989, **93**, 1713.
- 27 C. Jennings, R. Aroca, A. M. Hor and R. O. Loufty, *Spectrochim. Acta, Part A*, 1985, **41**, 1095.
- 28 T. Saito, W. Sisk, T. Kobayashi, S. Suzuki and T. Iwayanagi, *J. Phys. Chem.*, 1993, **97**, 8026.
- 29 J. P. Collman, C. E. Barnes, P. N. Swepston and J. A. Ibers, *J. Am. Chem. Soc.*, 1984, **106**, 3500.
- 30 A. R. Kane, J. F. Sullivan, D. H. Kenny and M. E. Kenney, *Inorg. Chem.*, 1970, **9**, 1445.
- 31 J. Mizuguchi, G. Rihs and H. R. Karfunkel, *J. Phys. Chem.*, 1995, **99**, 16217.